

# Where Do Flow Semantics Reside? A Protocol-Native Tabular Pretraining Paradigm for Encrypted Traffic Classification

Sizhe Huang<sup>1</sup> Shujie Yang<sup>1</sup>

## Abstract

Self-supervised masked modeling shows promise for encrypted traffic classification by masking and reconstructing raw bytes. Yet recent work reveals these methods fail to reduce reliance on labeled data despite costly pretraining: under frozen encoder evaluation, accuracy drops from  $>90\%$  to  $<47\%$ . We argue the root cause is **inductive bias mismatch**: flattening traffic into byte sequences destroys protocol-defined semantics. We identify three specific issues: 1) field unpredictability, random fields like `ip.id` are unlearnable yet treated as reconstruction targets; 2) embedding confusion, semantically distinct fields collapse into a unified embedding space; 3) metadata loss, capture-time metadata essential for temporal analysis is discarded. To address this, we propose a **protocol-native** paradigm that treats protocol-defined field semantics as architectural priors, reformulating the task to align with the data’s intrinsic tabular modality rather than incrementally adapting sequence-based architectures. Instantiating this paradigm, we introduce FlowSem-MAE, a tabular masked autoencoder built on Flow Semantic Units (FSUs). It features predictability-guided filtering that focuses on learnable FSUs, FSU-specific embeddings to preserve field boundaries, and dual-axis attention to capture intra-packet and temporal patterns. FlowSem-MAE significantly outperforms state-of-the-art across datasets. With only 50% labeled data, it outperforms most existing methods trained on full data.

## 1. Introduction

Encrypted traffic classification (ETC) has become essential for network security and management, as over 95% of

<sup>1</sup>State Key Laboratory of Networking and Switching Technology, Beijing University of Posts and Telecommunications, Beijing, China. Corresponding Author: Shujie Yang <sjyang@bupt.edu.cn>.

Preprint. March 12, 2026.

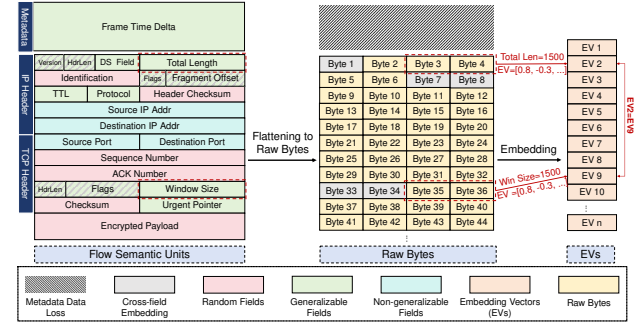


Figure 1. Protocol fields (left) are flattened into raw bytes (middle) and embedded (right), illustrating inductive bias mismatch at three levels: (P1) Field-level unpredictability: Random fields (pink) are treated as learnable despite being unpredictable by protocol design (e.g., `ip.id` and `checksum`). (P2) Cross-field-level embedding confusion: Field distinctions are lost through cross-field embedding (grey), where adjacent bytes span multiple fields (e.g., `ip.flags` and `ip.frag_offset`), and unified embedding function, where semantically different values receive identical vectors (e.g., `Total Len=1500` and `Win Size=1500`). (P3) Flow-level metadata loss: Temporal metadata (hatched) essential for flow-level behavior analysis exists outside packet bytes and is entirely discarded.

web traffic is now encrypted (Google, 2025) and traditional payload-based inspection is no longer viable. Recently, self-supervised masked modeling has been widely adopted for ETC, treating packets as generic byte sequences and reconstructing randomly masked bytes (Lin et al., 2022; Zhao et al., 2023; Wang et al., 2024). While this paradigm thrives in vision and NLP (Berahmand et al., 2024; Salazar et al., 2020; Hondru et al., 2025)—where the basic units (patches, tokens) naturally align with semantic structure—it remains questionable for encrypted traffic. However, *raw bytes often act as fragmented carriers rather than cohesive semantic units, leading to a fundamental misalignment between the masking objective and true flow semantics.*

### 1.1. Motivation: Limited Transferability

Existing byte-level masked modeling struggles to learn transferable representations for ETC. Under frozen encoder evaluation, a standard protocol for assessing representation quality, accuracy drops from over 90% (with full fine-tuning)

to below 47% (with frozen encoder), suggesting that pre-training contributes minimally to reduce reliance on labeled data (Zhao et al., 2025). The seemingly high accuracy of prior methods results from supervised fine-tuning, rather than from learned representations.

We argue that the root cause is **inductive bias mismatch**: byte-level modeling destroys the inherent semantics that network protocols explicitly define. Flattening this structured representation into raw bytes inevitably causes semantic loss at multiple levels.

We trace this mismatch to three fundamental issues (Fig. 1), which we refer to as P1-P3 for brevity:

**P1: Field-Level Unpredictability.** Not all protocol fields carry learnable signals. RFC 6274 recommends pseudo-random generation for `ip.id` to prevent information leakage (Gont, 2011), and RFC 9293 requires the initial sequence number to be “unpredictable to attackers” (Eddy, 2022). These fields are unlearnable by design, yet byte-based masking treats them as reconstruction targets, creating gradient noise that corrupts learning of meaningful fields.

**P2: Cross-Field-Level Embedding Confusion.** Byte-level modeling projects semantically distinct protocol fields through a unified embedding function, causing *cross-field pollution* and *value collision*. Unlike natural language polysemy where context disambiguates meaning, protocol fields are categorically distinct by specification (Yin et al., 2020). Positional encoding cannot resolve this issue, as it provides location information but lacks field-type awareness. From a manifold perspective (Brahma et al., 2015; Kienitz et al., 2022), each field type should occupy its own subspace, but shared embeddings collapse these into entangled regions.

**P3: Flow-Level Metadata Loss.** Byte-level methods operate solely on packet content, discarding capture-time metadata recorded by traffic analysis tools. Critical temporal features such as inter-arrival times (`frame.time_delta`) are essential for characterizing flow-level behaviors like burst patterns and request-response latency, yet they exist outside packet bytes and are entirely lost.

### 1.2. Key Insight: Protocol-Native Modeling

Encryption renders payloads unreadable, forcing classification to rely exclusively on protocol headers and metadata. As shown in Table 1, these elements form inherently *tabular data*: their dimensions and semantics are fixed by protocol specifications (Gont, 2011; Rescorla, 2018; Eddy, 2022). Prior methods assume flow semantics reside in byte sequences, but they actually reside in protocol-defined tabular structures—this modality mismatch explains why existing approaches fail to learn transferable representations. The core issue is not learning more, but learning right: aligning the learning paradigm with the data’s true modality is

Table 1. Network traffic as tabular data: mapping between tabular concepts and traffic elements.

Tabular Concept	Traffic Element
Table	Network flow (5-tuple session)
Row	Packet
Column	Protocol field
Column type	Field semantics
Row ordering	Temporal sequence

essential for capturing robust semantics.

To address this, we advocate a protocol-native paradigm that fundamentally reframes how to model encrypted traffic. Just as cloud-native designs systems around cloud infrastructure rather than adapting legacy architectures, **protocol-native treats protocol-defined field semantics as immutable priors, where structure is incorporated into model design rather than learned from data.** By operating on this intrinsic modality rather than flattened byte sequences, the paradigm ensures model inductive biases align with where flow semantics truly reside.

We instantiate this paradigm as FlowSem-MAE (Flow Semantics Masked Autoencoder), which operates on Flow Semantic Units (FSUs) through predictability-guided filtering (P1), FSU-specific embeddings (P2), and dual-axis attention (P3). These designs empirically validate that protocol-native modeling successfully captures transferable flow semantics.

Our contributions are as follows:

#### 1) Inductive Bias Analysis of Limited Transferability.

This analysis fundamentally reveals that the poor transferability of existing methods as resulting from inductive bias mismatch: modeling traffic as byte sequences obscures the semantics embedded in protocol-defined tabular structures. Solving this requires reformulating the task to align with the data’s intrinsic tabular modality, rather than incrementally adapting sequence-based architectures.

#### 2) Protocol-Native Paradigm.

We introduce a protocol-native paradigm, instantiated as FlowSem-MAE, a tabular pretraining framework that treats traffic flows as tabular data rather than byte sequences. By aligning the model architecture with protocol principles, it can effectively capture transferable representations robust to scenario shifts.

#### 3) Superior Performance.

FlowSem-MAE uniquely excels under both frozen encoder and full fine-tuning evaluation protocols, achieving the best or second-best performance across all metrics. With only 50% labeled data, it outperforms most existing methods trained on full data. We provide the code and model parameters in the supplementary material.

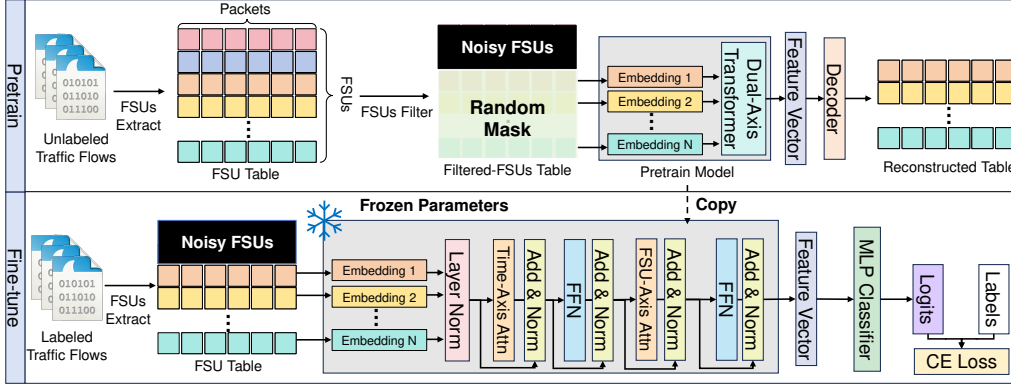


Figure 2. Workflow of FlowSem-MAE. Noisy FSUs refer to the union of random and non-generalizable fields.

## 2. Related Work

### 2.1. Statistical and Expert-Based Approaches

Traditional ETC methods rely on handcrafted features designed by network experts. Early approaches extract statistical features such as packet size distributions, flow duration (Finsterbusch et al., 2013). Deep Packet Inspection (DPI) analyzes protocol headers and payloads but becomes ineffective under encryption (Bujlow et al., 2015).

These methods suffer from poor scalability: feature engineering requires extensive manual effort and cannot adapt to rapidly evolving applications. These limitations motivate representation learning approaches that automatically extract features from raw traffic data.

### 2.2. Masked Language Modeling for Traffic

Inspired by BERT’s success in NLP (Devlin et al., 2019), recent work treats packets as sentences and bytes as tokens, applying masked language modeling to learn traffic representations (Lin et al., 2022; He et al., 2020; Zhou et al., 2025). ET-BERT (Lin et al., 2022) masks random bytes and reconstructs them from context, assuming that traffic bytes exhibit predictable patterns similar to natural language. TrafficFormer (Zhou et al., 2025) extends this with flow-level pretext tasks. Pcap-Encoder (Zhao et al., 2025) adopts a different strategy, using T5 (Ni et al., 2022) with question-answering pretraining specifically on protocol headers.

However, the core assumption that bytes behave like linguistic tokens is flawed: encrypted traffics lack the contextual regularities of natural language, and byte-level tokenization breaks protocol field boundaries.

### 2.3. Masked Vision Modeling for Traffic

Recent work converts packet sequences into 2D images and applies masked vision modeling (Hondru et al., 2025). YaTC (Zhao et al., 2023) represents flows as traffic matrices

and uses Vision Transformers with patch-based masking. NetMamba (Wang et al., 2024) employs the Mamba architecture for efficient sequence modeling.

These methods assume that traffic images exhibit spatial locality similar to natural images. However, unlike images where neighboring pixels correlate due to object continuity, traffic bytes from different protocol fields may be spatially adjacent but semantically unrelated.

### 2.4. Rethinking Traffic Representation Learning

Recent work has questioned the effectiveness of these approaches. Zhao et al. (2025) demonstrates that under frozen encoder evaluation, existing self-supervised learning methods exhibit severe performance degradation, and reveals that previously reported high accuracy stems from data leakage rather than learned representations.

Our work goes further by answering *why* pretrained representations fail to transfer. We identify inductive bias mismatch as the root cause: flow semantics reside in protocol-defined tabular structures, not byte sequences.

## 3. Method

### 3.1. Framework Overview

FlowSem-MAE is a protocol-native masked autoencoder that preserves flow semantics by using FSUs as modeling units, directly leveraging the semantics defined by RFCs.

**Problem Formulation.** Given a traffic flow  $\mathcal{F}$  consisting of  $T$  packets  $\{p_1, p_2, \dots, p_T\}$ , we extract  $N$  FSUs from each packet, forming a tabular flow representation  $\mathbf{X} = [x_i^t]_{T \times N}$  where  $x_i^t$  denotes the  $i$ -th FSU in packet  $t$  as a  $T \times N$  multi-row table. Our goal is to learn an encoder  $f_\theta : \mathbb{R}^{T \times N} \rightarrow \mathbb{R}^d$  that maps traffic flows to discriminative representations for downstream classification tasks.

**Architecture Overview.** As illustrated in Fig. 2, FlowSem-

MAE consists of four components: (1) FSU extraction that parses raw traffic into protocol fields and temporal metadata; (2) predictability-guided filtering that excludes unpredictable FSUs based on protocol priors; (3) FSU-specific embeddings where each FSU type has its own embedding function; and (4) a dual-axis Transformer that models both field relationships and temporal patterns. During pretraining, masked FSUs are reconstructed with:

$$\mathcal{L}_{\text{pretrain}} = \frac{1}{|\mathcal{M}_p|} \sum_{(t,i) \in \mathcal{M}_p} \ell(\hat{x}_i^t, x_i^t) \quad (1)$$

where  $\mathcal{M}_p$  denotes masked positions and  $\ell$  is the Mean Squared Error (MSE) loss. For downstream tasks, we freeze the encoder and train only the classification head to evaluate representation quality.

### 3.2. FSU Extraction and Preprocessing

**Flow Semantic Units.** Raw bytes ignore the inherent structure defined by protocol specifications, where each header field carries distinct semantics governed by RFCs. To preserve this structure, we extract FSUs from two sources: frame metadata and protocol headers.

Frame metadata includes temporal information such as inter-arrival time (`frame.time_delta`). Protocol headers include fields from IP and transport layers. In total, we extract 41 FSUs per packet after filtering random and non-generalizable fields.

**Flow Sampling.** Different phases of a network flow exhibit distinct behavioral patterns: connection establishment contains protocol handshake signatures, while termination reveals closing behaviors. To capture both phases, we sample the first 10 packets from each flow, yielding  $T = 10$  packets per flow. This strategy captures handshake patterns at flow start. Flows shorter than 10 packets are padded with a mask indicating valid positions.

**Feature Normalization.** Protocol fields have heterogeneous value ranges and distributions, requiring type-specific normalization to ensure numerical comparability while preserving semantics. Unlike traditional expert-based approaches that manually design statistical features (e.g., mean packet size, flow duration), our normalization preserves the original semantic meaning of each field. This allows the model to automatically learn discriminative patterns through pretraining rather than relying on predefined features.

### 3.3. Predictability-Guided Filtering

Byte-level MAE methods treat all bytes as potential reconstruction targets, forcing models to predict inherently random fields alongside meaningful ones. This creates noisy gradients that corrupt the entire representation space. Clas-

sifiers can learn to ignore noisy features, but masked autoencoding explicitly supervises masked positions. When these include unpredictable fields, the model is forced to predict random values, creating gradient noise that corrupts learning. We exclude such FSUs based on RFCs to preserve field-level semantics.

**Protocol Prior Analysis.** We categorize FSUs into three types based on predictability. Let  $N$  denote the number of FSU types, and  $\mathcal{S} = \{s_1, s_2, \dots, s_N\}$  denote the set of FSU types, partitioned into:  $\mathcal{S}_g$  (generalizable) with stable, learnable patterns;  $\mathcal{S}_r$  (random) generated by cryptographic operations or integrity checks; and  $\mathcal{S}_n$  (non-generalizable) containing dataset-specific fields.

- *Random FSUs* are fields that lack learnable patterns due to cryptographic operations, system implementations, or integrity checks (Gont, 2011; Rescorla, 2018). They are excluded from pretraining.
- *Non-generalizable FSUs* are dataset-specific fields that may cause overfitting, including source and destination IP addresses. These fields are excluded to prevent the model from learning spurious correlations.
- *Generalizable FSUs* are fields with stable, learnable patterns governed by protocol specifications or reflecting meaningful traffic characteristics. These fields serve as reconstruction targets during pretraining.

**Dual Masking Strategy.** To capture both temporal dependencies and semantic structure, we employ two complementary masks  $m_{\text{packet}}^t$  and  $m_{\text{field}}^i$ , each sampled from a Bernoulli distribution. *Packet-level masking* ( $m_{\text{packet}}^t = 1$ ) masks all FSUs at time  $t$ , encouraging the model to predict from neighboring packets. *Field-level masking* ( $m_{\text{field}}^i = 1$ ) masks FSU  $i$  across all packets, encouraging inference from other fields within each packet.

Random and Non-Generalizable FSUs ( $i \in \mathcal{S}_r \cup \mathcal{S}_n$ ) are excluded entirely and never serve as reconstruction targets. This selective mechanism addresses **P1** by focusing learning capacity on FSUs with stable, generalizable patterns.

### 3.4. FSU-Specific Embeddings

Byte-based methods project all bytes through a shared embedding function, conflating semantically distinct fields. Crucially, *positional encoding* (Vaswani et al., 2017) cannot resolve this issue. While position embeddings distinguish byte locations (e.g., byte 9 vs. byte 33), they cannot capture field semantics: the same value at different positions (e.g., TTL=128 at byte 9, Len=128 at byte 3) should have *different* meanings, while different values of the same field (e.g., TTL=64 vs. TTL=128) should share semantic structure.

To preserve FSU-specific semantics, we assign each FSU type its own embedding function with independent parameters, inspired by tabular representation learning (Gorishniy et al., 2021). This acknowledges that different protocol fields carry distinct semantics.

We define type-specific embedding functions  $\{E_1, \dots, E_N\}$  where  $E_k : \mathbb{R} \rightarrow \mathbb{R}^d$  maps FSU type  $k$ 's values to  $d$ -dim vectors:

$$E_k(x_i^t) = \mathbf{W}_k x_i^t + \mathbf{b}_k \quad (2)$$

where  $\mathbf{W}_k \in \mathbb{R}^{d \times 1}$  and  $\mathbf{b}_k \in \mathbb{R}^d$  are FSU-specific parameters. The complete embedding combines value embedding with positional encodings:

$$\mathbf{e}_i^t = E_{k_i}(x_i^t) + \mathbf{p}_i + \mathbf{q}_t \quad (3)$$

where  $\mathbf{p}_i$  is FSU position encoding and  $\mathbf{q}_t$  is temporal position encoding. This contrasts with byte-level methods that use a single shared projection  $E(x) = \mathbf{W}x + \mathbf{b}$  for all fields, which maps identical values from different FSU types to identical representations. This design addresses **P2** by preserving cross-field-level semantics through maintaining semantic boundaries across protocol fields.

**Manifold Preservation.** Under the manifold hypothesis (Fefferman et al., 2016), network traffic features lie on low-dimensional manifolds  $\{\mathcal{M}_k\}_{k=1}^N$ , where each FSU type  $k$  exhibits distinct geometric structure. For instance, TTL values concentrate on discrete points  $\{64, 128, 255\}$ , while inter-arrival times follow a continuous distribution.

Shared embeddings  $E : \bigcup_k \mathcal{M}_k \rightarrow \mathbb{R}^d$  induce *manifold entanglement* (Brahma et al., 2015), where geometrically distinct structures collapse into overlapping regions. When embedding capacity is insufficient ( $d < \sum_k d_k$ ), this entanglement is unavoidable, causing severe variance imbalance across FSU types.

FSU-specific embeddings  $\{E_k\}_{k=1}^N$  preserve manifold separation through independent parameterization for each field type. This design empirically achieves near-zero entanglement and eliminates cross-field semantic confusion, enabling the encoder to learn FSU-specific patterns without interference.

### 3.5. Dual-Axis Transformer Architecture

Standard Transformers process sequences with single-axis attention, treating input as a flat sequence (Han et al., 2022). However, traffic flows exhibit an inherent two-dimensional structure: temporal patterns across packets and semantic relationships among FSUs within each packet. To capture both dimensions effectively, we employ dual-axis attention.

**Dual-Axis Attention.** FlowSem-MAE employs dual-axis attention on the representation  $\mathbf{E} \in \mathbb{R}^{T \times N \times d}$ .

*Time-axis attention* models dependencies across  $T$  packets for each FSU position, capturing how individual fields evolve over the flow's lifetime:

$$\mathbf{H}_{\text{time}} = \text{MultiheadAttn}(\mathbf{Q}_{\text{time}}, \mathbf{K}_{\text{time}}, \mathbf{V}_{\text{time}}) \quad (4)$$

*FSU-axis attention* models dependencies across  $N$  FSUs within each packet, capturing inter-field relationships:

$$\mathbf{H}_{\text{fsu}} = \text{MultiheadAttn}(\mathbf{Q}_{\text{fsu}}, \mathbf{K}_{\text{fsu}}, \mathbf{V}_{\text{fsu}}) \quad (5)$$

While FSU-axis attention performs standard intra-packet modeling, time-axis attention addresses **P3** by preserving flow-level semantics through explicitly capturing inter-packet temporal dependencies over the capture-time metadata (e.g., `frame.time_delta`) included in FSUs, enabling the model to learn flow-level behavioral patterns such as request-response latency and burst characteristics. Note that TCP header timestamps (TSval/TSecr) cannot substitute for capture-time metadata, as they reflect sender clocks rather than arrival times.

**Encoder Architecture.** The encoder consists of  $L$  transformer blocks, each applying time-axis attention, FSU-axis attention, and feed-forward networks with layer normalization and residual connections:

$$\mathbf{H}_{\text{time}}^\ell = \text{TimeAttn}(\text{LN}(\mathbf{H}^{\ell-1})) + \mathbf{H}^{\ell-1} \quad (6)$$

$$\tilde{\mathbf{H}}^\ell = \text{FFN}(\text{LN}(\mathbf{H}_{\text{time}}^\ell)) + \mathbf{H}_{\text{time}}^\ell \quad (7)$$

$$\mathbf{H}_{\text{fsu}}^\ell = \text{FSUAttn}(\text{LN}(\tilde{\mathbf{H}}^\ell)) + \tilde{\mathbf{H}}^\ell \quad (8)$$

$$\mathbf{H}^\ell = \text{FFN}(\text{LN}(\mathbf{H}_{\text{fsu}}^\ell)) + \mathbf{H}_{\text{fsu}}^\ell \quad (9)$$

For downstream classification, we apply mean pooling over time and FSU dimensions to obtain flow representation  $\mathbf{z} \in \mathbb{R}^d$ , followed by an MLP classification head.

## 4. Experiments

### 4.1. Experimental Setup

**Datasets.** For pretraining, we use MAWI traffic traces from January 1, 2025 (Cho et al., 2000) (137M packets, 9.6GB) with no overlap with evaluation datasets. We evaluate on **ISCX-VPN** (Gil et al., 2016) (16 application classes) and **CSTNET-TLS 1.3 (i.e., TLS-120)** (Lin et al., 2022) (120 website classes with SNI removed, encrypted by TLS 1.3).

**Data Preparation.** Following Zhao et al. (2025), we remove extraneous protocols (ARP, DHCP, etc.). Due to the high IP homogeneity within application labels, we anonymize IP addresses to prevent spurious correlations for all methods.

**Baselines.** We compare against six pretrained models spanning diverse architectures: **ET-BERT** (Lin et al., 2022) and **Pcap-Encoder** (Zhao et al., 2025) are byte-based methods

Table 2. Performance comparison with frozen encoders. Best results in **bold**, second best underlined.

Model	ISCX-VPN		TLS-120	
	Acc	F1	Acc	F1
Pcap-Encoder	16.1	12.1	7.1	2.9
ET-BERT	22.3	12.8	9.1	4.6
NetMamba	15.6	13.6	16.9	11.3
netFound	22.9	18.8	28.0	22.9
YaTC	37.5	34.6	34.1	27.6
TrafficFormer	<u>39.2</u>	<u>36.9</u>	<u>46.3</u>	<u>42.3</u>
<b>FlowSem-MAE</b>	<b>51.1</b>	<b>42.7</b>	<b>55.2</b>	<b>51.3</b>

applying BERT-style pretraining; **YaTC** (Zhao et al., 2023) and **NetMamba** (Wang et al., 2024) are vision-based methods using masked image modeling; **TrafficFormer** (Zhou et al., 2025) and **netFound** (Guthula et al., 2023) are hybrid methods incorporating flow-level pretext tasks. Flow-based encoders process 10 packets jointly; packet-based encoders use majority voting.

**Evaluation.** We use **frozen encoder evaluation** (Zhao et al., 2025): only the classification head is trained while encoder weights remain fixed. This stringent protocol isolates the contribution of pretraining from fine-tuning, testing whether pretraining truly learns transferable features.

### 4.2. Main Results

Table 2 presents the frozen encoder performance. FlowSem-MAE significantly outperforms all baselines on both datasets, achieving 51.1% accuracy and 42.7% Macro-F1 on ISCX-VPN, surpassing TrafficFormer by 11.9% and 5.8% respectively. On TLS-120, FlowSem-MAE achieves 55.2% accuracy and 51.3% Macro-F1, outperforming TrafficFormer by 8.9% and 9.0%. These improvements validate that preserving flow semantics through protocol-native modeling produces genuinely transferable representations.

Byte-based methods (Pcap-Encoder, ET-BERT) perform poorly because they attempt to learn from encrypted payloads with no learnable patterns. Vision-based methods (YaTC, NetMamba) achieve moderate results, but patch-based tokenization still conflates semantically distinct protocol fields. TrafficFormer emerges as the strongest baseline due to its flow-level pretext tasks, yet still falls short without addressing field-level semantics. The discrepancy between our results and those in Zhao et al. (2025) is due to IP anonymization.

**Model Efficiency.** Fig. 3 illustrates the relationship between model size and performance. Larger models do not yield better representations: netFound (2.85B parameters, 57× larger than ours) achieves only 18.8% and 22.9% F1; Pcap-

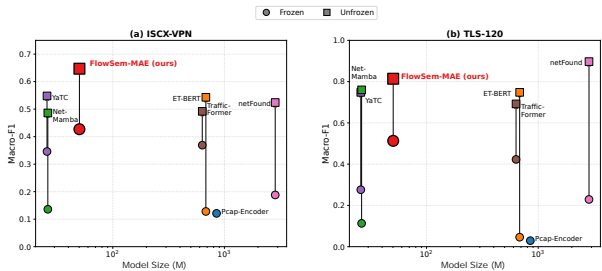


Figure 3. Model size vs. performance (Macro-F1). FlowSem-MAE achieves the best performance with only 50.25M model size, significantly outperforming larger models.

Table 3. Frozen (Fro.) vs. Unfrozen (Unfro.) performance comparison (Macro-F1).

Model	ISCX-VPN		TLS-120	
	Fro.	Unfro.	Fro.	Unfro.
ET-BERT	12.8	54.3	4.6	51.5
NetMamba	13.6	48.6	11.3	76.0
netFound	18.8	52.4	22.9	<b>89.7</b>
YaTC	34.6	<u>54.8</u>	27.6	74.8
TrafficFormer	<u>36.9</u>	49.2	<u>42.3</u>	69.2
<b>FlowSem-MAE</b>	<b>42.7</b>	<b>68.5</b>	<b>51.3</b>	<u>83.8</u>

Encoder (850M) and ET-BERT (682M) perform poorly despite substantial sizes. FlowSem-MAE achieves the best performance with only 50.25M model size, demonstrating that aligning pretraining with traffic’s tabular structure matters more than model scale.

### 4.3. Transferability Analysis

To validate that FlowSem-MAE learns genuinely transferable representations, we compare frozen and unfrozen (full fine-tuning) performance in Table 3. A well-pretrained model should excel under *both* protocols: frozen performance measures representation quality in isolation, while unfrozen performance measures the foundation it provides for task-specific adaptation. **FlowSem-MAE uniquely excels under both evaluation protocols.** Our method achieves the best frozen performance on both datasets (42.7% and 51.3% F1) *and* the best or second-best unfrozen performance (68.5% and 83.8% F1). This dual excellence is unique among all methods and demonstrates that FSU-based pretraining learns representations that are both independently discriminative and amenable to further adaptation.

Baselines fall into two failure modes: (1) *Collapse when frozen*: ET-BERT and netFound achieve reasonable unfrozen performance but collapse under frozen evaluation (4.6% and 22.9% F1 on TLS-120), indicating their pre-

Table 4. Ablation study on FlowSem-MAE components.

Variant	ISCX-VPN		TLS-120	
	Acc	F1	Acc	F1
<b>FlowSem-MAE (full)</b>	<b>51.1</b>	<b>42.7</b>	<b>55.2</b>	<b>51.3</b>
w/o Pred-Guided Filter	27.9	17.3	34.8	29.8
w/o FSU-Spec Embed	40.8	16.5	25.9	21.3
w/o Temporal Metadata	45.3	30.5	44.7	39.5

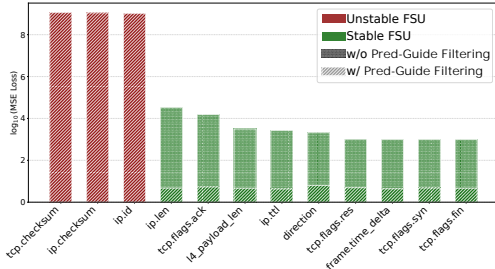


Figure 4. Effect of predictability-guided filtering on reconstruction loss. Without predictability-guided filtering, random fields (red) exhibit extremely high loss ( $\sim 10^9$ ) and degrade learning of generalizable fields (green).

training contributes minimally—performance gains come entirely from fine-tuning on labeled data. (2) *Plateau when unfrozen*: TrafficFormer shows the second-best frozen performance but fails to improve proportionally when unfrozen (42.3%→69.2% on TLS-120), suggesting its representations are less adaptable. FlowSem-MAE breaks this trade-off: strong frozen performance (51.3%) translates into strong unfrozen performance (83.8%), confirming that FSU-based pretraining provides both a solid standalone representation and an effective initialization for fine-tuning.

**Model size efficiency.** While netFound requires 2.85B to achieve 89.7% unfrozen F1 on TLS-120, its frozen F1 is only 22.9%. FlowSem-MAE achieves 83.8% unfrozen F1 and 51.3% frozen F1 with  $57\times$  fewer. The 5.9% unfrozen gap is minor compared to the 28.4% frozen improvement, validating that matching masked units to data structure matters more than model scale.

#### 4.4. Ablation Study

To validate the contribution of each component, we conduct ablation experiments (Table 4).

**Impact of Predictability-Guided Filtering (P1).** Removing predictability-guided filtering causes 23.2% and 20.4% accuracy drop on ISCX-VPN and TLS-120 respectively. Fig. 4 reveals the mechanism: forcing the model to reconstruct random fields (checksums, IDs) results in extremely high loss ( $\sim 10^9$ ) and degrades reconstruction quality across all generalizable fields, confirming that random fields create

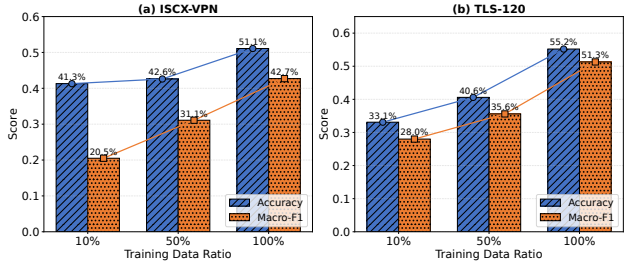


Figure 5. Performance under different labeled data ratios.

noisy gradients corrupting the entire representation space.

**Impact of FSU-Specific Embeddings (P2).** When replacing FSU-specific embeddings with a single shared linear projection, the severe degradation confirms that shared embeddings cause cross-field semantic pollution; fine-grained field semantics are crucial for distinguishing TLS-encrypted websites.

**Impact of Temporal Metadata (P3).** Removing temporal information reduces accuracy by 5.8% and 10.5% on ISCX-VPN and TLS-120, with Macro-F1 drops of 12.2% and 11.8% respectively. This demonstrates that inter-packet temporal patterns are essential for flow-level classification.

#### 4.5. Label Efficiency

To evaluate robustness under limited labeled data, we vary the labeled data ratio from 10% to 100% (Fig. 5). FlowSem-MAE demonstrates strong performance even with scarce labels: 41.3% accuracy on ISCX-VPN with only 10% data (80.8% of full performance). Notably, with 50% labeled data, FlowSem-MAE achieves performance comparable to TrafficFormer with full data, demonstrating that pretraining learns transferable representations that substantially reduce labeling requirements.

#### 4.6. Embedding Space Analysis

To validate the manifold preservation property of FSU-specific embeddings, we analysis the embedding space between our approach and shared embeddings (Fig. 6).

**Results.** FSU-specific embeddings exhibit two desirable properties. First, inter-FSU centroid distances are uniformly distributed (0.4–0.8 for most pairs), indicating appropriate separation without extreme clustering or dispersion. Second, intra-FSU variances are uniformly low ( $\sim 0.0007$ ), showing each FSU forms a compact cluster through its independent embedding function.

In contrast, shared embeddings suffer from severe *manifold entanglement*. The distance matrix exhibits a block structure: most FSU pairs show near-zero distances ( $< 0.25$ ), collapsing into overlapping regions, while a few FSUs are

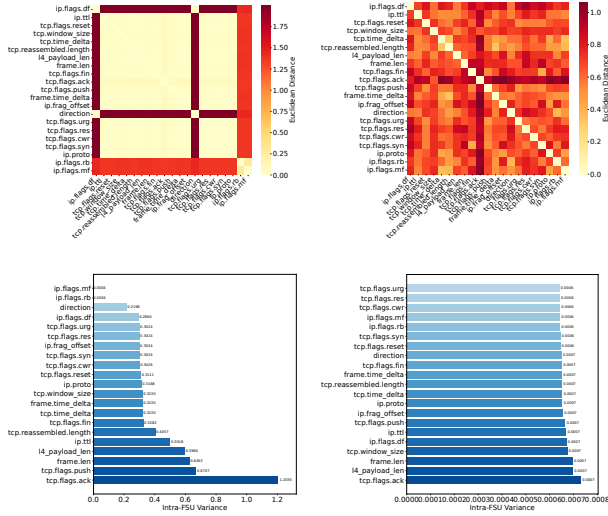


Figure 6. Embedding space analysis. Top: Inter-FSU centroid distances; Bottom: Intra-FSU variance. Left: Shared embeddings; Right: FSU-specific embeddings. FSU-specific embeddings achieve uniform separation (0.4–0.8) and consistent compactness (~0.0007), while shared embeddings show extreme distances (0–1.75) and 3000× variance disparity.

extremely distant (>1.5). This bimodal pattern reveals a “rich-get-richer” phenomenon: FSUs with stronger gradients cluster with well-learned representations, while low-gradient FSUs remain near random initialization. More critically, intra-FSU variances differ by 3000×, showing shared embeddings fail to provide consistent representation quality. FSU-specific embeddings resolve both issues through independent parameterization for each field type.

### 4.7. FSU Importance Analysis

A key advantage of FSU-based modeling is interpretability. We measure FSU importance via gradient-based attribution and compare with XGBoost feature importance (Fig. 7).

The results show moderate-to-strong positive correlation (Spearman  $\rho = 0.536$  on ISCX-VPN,  $\rho = 0.696$  on TLS-120). Top-ranked FSUs differ between datasets: `direction`, `ack`, and `df` dominate on ISCX-VPN, reflecting that VPN-encrypted applications are distinguished by flow directionality and TCP flags; `df` ranks highest on TLS-120, indicating website fingerprinting relies more on protocol-level signatures.

The moderate rather than perfect correlation is expected—XGBoost operates on individual values independently, while FlowSem-MAE captures interactions via dual-axis attention. Notable divergences support this: `len` ranks 9th for FlowSem-MAE but highest for XGBoost on ISCX-VPN, suggesting packet length is individually discriminative but our model discovers richer patterns; `syn` ranks 5th vs.

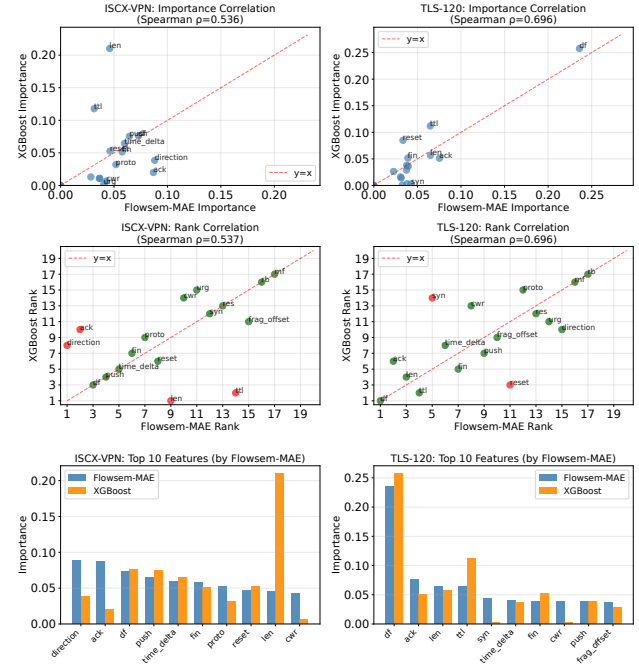


Figure 7. FSU importance comparing FlowSem-MAE with XGBoost. Moderate-to-strong Spearman correlation ( $\rho = 0.536$  on ISCX-VPN,  $\rho = 0.696$  on TLS-120) indicates FlowSem-MAE discovers similar discriminative features while capturing additional interaction patterns.

15th on TLS-120, indicating connection establishment becomes discriminative only when modeled across sequences. The consistency validates meaningful representations; the divergence demonstrates capacity to model higher-order patterns invisible to feature-independent methods.

## 5. Conclusion

**Implications.** We identify the inductive bias mismatch as the root cause of poor transferability in traffic classification. We propose a protocol-native paradigm that aligns with the intrinsic tabular modality of network data, instantiated by FlowSem-MAE. Leveraging Flow Semantic Units and dual-axis attention, our approach demonstrates that structural semantic alignment outperforms brute-force model scaling, even with limited labeled data. We establish a foundation for semantically grounded, protocol-native traffic analysis.

**Limitations.** While effective, accuracy can be further improved with larger pretraining datasets. Additionally, manual field categorization for predictability-guided filtering could be automated via information-theoretic methods.

## References

Berahmand, K., Daneshfar, F., Salehi, E. S., Li, Y., and Xu, Y. Autoencoders and their applications in machine

- learning: a survey. *Artificial intelligence review*, 57(2): 28, 2024.
- Brahma, P. P., Wu, D., and She, Y. Why deep learning works: A manifold disentanglement perspective. *IEEE transactions on neural networks and learning systems*, 27(10):1997–2008, 2015.
- Bujlow, T., Carela-Español, V., and Barlet-Ros, P. Independent comparison of popular dpi tools for traffic classification. *Computer Networks*, 76:75–89, 2015. ISSN 1389-1286. doi: <https://doi.org/10.1016/j.comnet.2014.11.001>. URL <https://www.sciencedirect.com/science/article/pii/S1389128614003909>.
- Cho, K., Mitsuya, K., and Kato, A. Traffic data repository at the {WIDE} project. In *2000 USENIX Annual Technical Conference (USENIX ATC 00)*, 2000.
- Devlin, J., Chang, M.-W., Lee, K., and Toutanova, K. BERT: Pre-training of deep bidirectional transformers for language understanding. In Burstein, J., Doran, C., and Solorio, T. (eds.), *Proceedings of the 2019 Conference of the North American Chapter of the Association for Computational Linguistics: Human Language Technologies, Volume 1 (Long and Short Papers)*, pp. 4171–4186, Minneapolis, Minnesota, June 2019. Association for Computational Linguistics. doi: 10.18653/v1/N19-1423. URL <https://aclanthology.org/N19-1423/>.
- Eddy, W. Transmission Control Protocol (TCP). RFC 9293, August 2022. URL <https://www.rfc-editor.org/info/rfc9293>.
- Fefferman, C., Mitter, S., and Narayanan, H. Testing the manifold hypothesis. *Journal of the American Mathematical Society*, 29(4):983–1049, 2016.
- Finstelbusch, M., Richter, C., Rocha, E., Muller, J.-A., and Hanssgen, K. A survey of payload-based traffic classification approaches. *IEEE Communications Surveys & Tutorials*, 16(2):1135–1156, 2013.
- Gil, G. D., Lashkari, A. H., Mamun, M., and Ghorbani, A. A. Characterization of encrypted and vpn traffic using time-related features. In *Proceedings of the 2nd international conference on information systems security and privacy (ICISSP 2016)*, pp. 407–414. SciTePress Setúbal, Portugal, 2016.
- Gont, F. Security Assessment of the Internet Protocol Version 4. RFC 6274, July 2011. URL <https://www.rfc-editor.org/info/rfc6274>.
- Google. Https encryption on the web, 2025. URL <https://transparencyreport.google.com/https/overview>.
- Gorishniy, Y., Rubachev, I., Khrulkov, V., and Babenko, A. Revisiting deep learning models for tabular data. In Ranzato, M., Beygelzimer, A., Dauphin, Y., Liang, P., and Vaughan, J. W. (eds.), *Advances in Neural Information Processing Systems*, volume 34, pp. 18932–18943. Curran Associates, Inc., 2021. URL [https://proceedings.neurips.cc/paper\\_files/paper/2021/file/9d86d83f925f2149e9edb0ac3b49229c-Paper.pdf](https://proceedings.neurips.cc/paper_files/paper/2021/file/9d86d83f925f2149e9edb0ac3b49229c-Paper.pdf).
- Guthula, S., Beltiukov, R., Battula, N., Guo, W., and Gupta, A. netfound: Foundation model for network security. *arXiv preprint arXiv:2310.17025*, 2023.
- Han, K., Wang, Y., Chen, H., Chen, X., Guo, J., Liu, Z., Tang, Y., Xiao, A., Xu, C., Xu, Y., et al. A survey on vision transformer. *IEEE transactions on pattern analysis and machine intelligence*, 45(1):87–110, 2022.
- He, H. Y., Guo Yang, Z., and Chen, X. N. Pert: Payload encoding representation from transformer for encrypted traffic classification. In *2020 ITU Kaleidoscope: Industry-Driven Digital Transformation (ITU K)*, pp. 1–8, 2020. doi: 10.23919/ITUK50268.2020.9303204.
- Hondru, V., Croitoru, F., Minaee, S., Ionescu, R. T., and Sebe, N. Masked image modeling: A survey. *Int. J. Comput. Vis.*, 133(10):7154–7200, 2025. doi: 10.1007/S11263-025-02524-1. URL <https://doi.org/10.1007/s11263-025-02524-1>.
- Kienitz, D., Komendantskaya, E., and Lones, M. The effect of manifold entanglement and intrinsic dimensionality on learning. *Proceedings of the AAAI Conference on Artificial Intelligence*, 36(7):7160–7167, Jun. 2022. doi: 10.1609/aaai.v36i7.20676. URL <https://ojs.aaai.org/index.php/AAAI/article/view/20676>.
- Lin, X., Xiong, G., Gou, G., Li, Z., Shi, J., and Yu, J. Etbert: A contextualized datagram representation with pre-training transformers for encrypted traffic classification. In *Proceedings of the ACM Web Conference 2022, WWW '22*, pp. 633–642, New York, NY, USA, 2022. Association for Computing Machinery. ISBN 9781450390965. doi: 10.1145/3485447.3512217. URL <https://doi.org/10.1145/3485447.3512217>.
- Ni, J., Hernandez Abrego, G., Constant, N., Ma, J., Hall, K., Cer, D., and Yang, Y. Sentence-t5: Scalable sentence encoders from pre-trained text-to-text models. In Muresan, S., Nakov, P., and Villavicencio, A. (eds.), *Findings of the Association for Computational Linguistics: ACL 2022*, pp. 1864–1874, Dublin, Ireland, May 2022. Association for Computational Linguistics. doi: 10.18653/v1/2022.findings-acl.146. URL <https://aclanthology.org/2022.findings-acl.146/>.

- Rescorla, E. The Transport Layer Security (TLS) Protocol Version 1.3. RFC 8446, August 2018. URL <https://www.rfc-editor.org/info/rfc8446>.
- Salazar, J., Liang, D., Nguyen, T. Q., and Kirchhoff, K. Masked language model scoring. In Jurafsky, D., Chai, J., Schluter, N., and Tetreault, J. (eds.), *Proceedings of the 58th Annual Meeting of the Association for Computational Linguistics*, pp. 2699–2712, Online, July 2020. Association for Computational Linguistics. doi: 10.18653/v1/2020.acl-main.240. URL <https://aclanthology.org/2020.acl-main.240/>.
- Vaswani, A., Shazeer, N., Parmar, N., Uszkoreit, J., Jones, L., Gomez, A. N., Kaiser, Ł., and Polosukhin, I. Attention is all you need. *Advances in neural information processing systems*, 30, 2017.
- Wang, T., Xie, X., Wang, W., Wang, C., Zhao, Y., and Cui, Y. Netmamba: Efficient network traffic classification via pre-training unidirectional mamba. In *2024 IEEE 32nd International Conference on Network Protocols (ICNP)*, pp. 1–11. IEEE, 2024.
- Yin, P., Neubig, G., Yih, W.-t., and Riedel, S. TaBERT: Pretraining for joint understanding of textual and tabular data. In Jurafsky, D., Chai, J., Schluter, N., and Tetreault, J. (eds.), *Proceedings of the 58th Annual Meeting of the Association for Computational Linguistics*, pp. 8413–8426, Online, July 2020. Association for Computational Linguistics. doi: 10.18653/v1/2020.acl-main.745. URL <https://aclanthology.org/2020.acl-main.745/>.
- Zhao, R., Zhan, M., Deng, X., Wang, Y., Wang, Y., Gui, G., and Xue, Z. Yet another traffic classifier: A masked autoencoder based traffic transformer with multi-level flow representation. In *Proceedings of the AAAI Conference on Artificial Intelligence*, volume 37, pp. 5420–5427, 2023.
- Zhao, Y., Dettori, G., Boffa, M., Vassio, L., and Mellia, M. The sweet danger of sugar: Debunking representation learning for encrypted traffic classification. In *Proceedings of the ACM SIGCOMM 2025 Conference*, pp. 296–310, 2025.
- Zhou, G., Guo, X., Liu, Z., Li, T., Li, Q., and Xu, K. Trafficformer: an efficient pre-trained model for traffic data. In *2025 IEEE Symposium on Security and Privacy (SP)*, pp. 1844–1860. IEEE, 2025.